Olefin Dimerization and Isomerization Catalyzed by Pyridylidene Amide Palladium Complexes

Miquel Navarro,[†] Vera Rosar,[†,‡] Tiziano Montini,[‡] Barbara Milani,*[,‡] and Martin Albrecht*[,†]

[†]Department für Chemie und Biochemie, Universität Bern, CH−3012 Bern, Switzerland

[‡]Department of Chemical and Pharmaceutical Sciences, University of Trieste, via Licio Giorgieri 1, 34127 Trieste, Italy

Supporting Information

ABSTRACT: A series of cationic palladium complexes [Pd(N^N′)Me(NCMe)]$^+$ was synthesized, comprising three different N^N′-bidentate coordinating pyridyl−pyridylidene amide (PYA) ligands with different electronic and structural properties depending on the PYA position (*o*-, *m*-, and *p*-PYA). Structural investigation in solution revealed cis/trans isomeric ratios that correlate with the donor properties of the PYA ligand, with the highest cis ratios for the complex having the most donating *o*-PYA ligand and lowest ratios for that with the weakest donor *p*-PYA system. The catalytic activity of the cationic complexes [Pd(N^N′)Me(NCMe)]$^+$ in alkene insertion and dimerization showed a strong correlation with the ligand setting. While complexes bearing more electron donating *m*- and *o*-PYA ligands produced butenes within 60 and 30 min, respectively, the *p*-PYA complex was much slower and only reached 50% conversion of ethylene within 2 h. Likewise, insertion of methyl acrylate as a polar monomer was more efficient with stronger donor PYA units, reaching a 32% ratio of methyl acrylate vs ethylene insertion. Mechanistic investigations about the ethylene insertion allowed detection, for the first time, by NMR spectroscopy both *cis*- and *trans*-Pd-ethyl intermediates and, furthermore, revealed a trans to cis isomerization of the Pd-ethyl resting state as the rate-limiting step for inducing ethylene conversion. These PYA palladium complexes induce rapid double-bond isomerization of terminal to internal alkenes through a chain-walking process, which prevents both polymerization and also the conversion of higher olefins, leading selectively to ethylene dimerization.

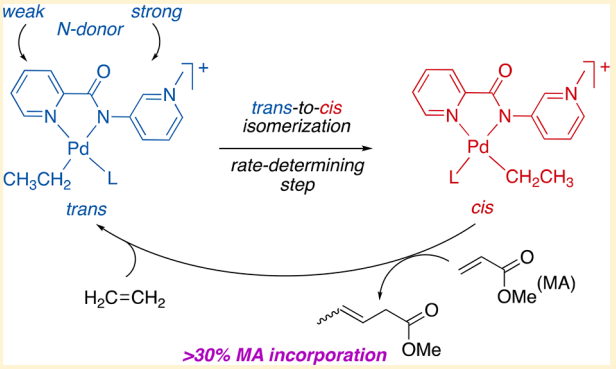

INTRODUCTION

Over the last decades substantial efforts have been devoted to develop late-transition-metal complexes as catalyst precursors for olefin polymerization reactions.[1] Late transition metals offer significant advantages over early transition metals for this reaction, as they typically demonstrate a high tolerance of functional groups because of their lower oxidation state and higher electronegativity, their inherently high robustness toward air and moisture, and their potential to polymerize at low temperatures.[2] Pioneering work by Brookhart and co-workers exploited the development of sterically shielded α-diimine palladium complexes (**A**, Figure 1) for ethylene homopolymerization.[3] This discovery opened the door to the use of Pd(II) complexes as catalysts for the copolymerization of ethylene with polar vinyl monomers to yield functionalized polyolefins. Building on this concept, Drent developed a series of P^O-bidentate ligands (**B**, Figure 1), which, in contrast to the Brookhart diimine systems, do not have C_2 symmetry, and demonstrated the impact of the diverging electronic effects of the two chelating sites in ethylene/alkyl acrylate copolymerization.[4] These pioneering studies instigated numerous research programs toward copolymerization with various polar vinyl monomers.[5] Our group has recently combined the two ligand design strategies by developing a family of C^N-bidentate ligands that feature elements of the α-diimine system (imine bonding through N-coordination of pyridine) and the ligand dissymmetry and strong donor properties of the phosphine by using an N-heterocyclic carbene (NHC) unit (**C**, Figure 1).[6] The corresponding (C^N)Pd complexes showed selective dimerization of ethylene when sterically demanding ligands were employed, while the absence of shielding bulky groups on the C^N-bidentate ligand resulted in the formation of propene and the imidazolium salt due to a reductive elimination process. More recently, Pd(II) and Ni(II) complexes with anionic C^O-bidentate NHC ligands (**D**, Figure 1) demonstrated catalytic activity in the copolymerization of ethylene or propene with alkyl acrylates[7] and allyl acetate, respectively.[8]

Since carbon-based ligands risk undergoing reductive elimination, in particular at the Pd−H stage formed in the chain termination step of the catalytic cycle, different strong donor ligand sites based on heteroatoms are highly desirable.

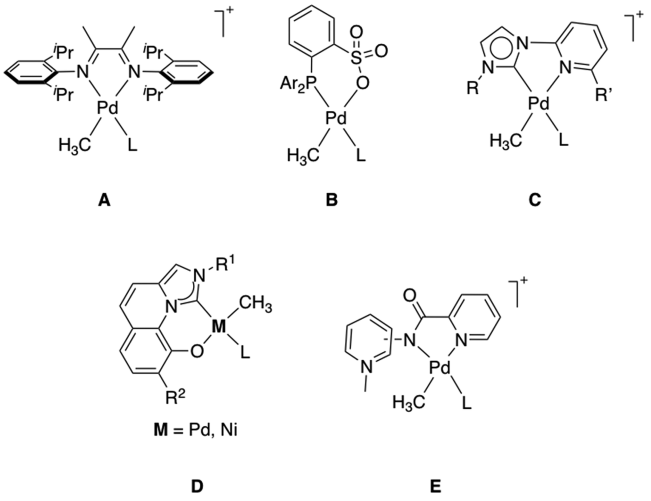

Figure 1. Copolymerization precatalysts based on palladium complexes with specific ligand motifs: α-diimine (**A**), P^O-bidentate phosphine sulfonate (**B**), sterically flexible NHC-imine (**C**), C^O-bidentate NHC alkoxide (**D**), and N^N′-chelating PYA-imine (**E**; this work).

Pyridylidene amides (PYAs) have been described as ligands with donor properties that parallel those of N-heterocyclic carbenes.[9] These properties, together with the versatility offered by the straightforward synthesis of this class of compounds, make them very promising candidates as ancillary ligands for catalytic applications. Indeed, recent work has shown that these ligands impart high catalytic activity when they are coordinated to platinum-group metals.[10] Therefore, we have now enlarged the set of N^N′-bidentate chelating ligands and designed the pyridyl-PYA systems **E** (Figure 1), which combine properties from both Brookhart's α-diimine and Drent's dissymmetric phosphine-sulfonate systems, with higher resistance toward reductive elimination in comparison to the NHC ligands. Herein, we report on the synthesis of palladium(II) complexes and their activity in terminal alkene dimerization. Mechanistic investigations indicate that these new PYA palladium complexes are very fast olefin isomerization catalysts, which effectively hampers polymer chain growth.

RESULTS AND DISCUSSION

Synthesis and Characterization of PYA Palladium Complexes. A series of PYA palladium complexes was prepared starting from picolinic acid in three straightforward synthetic steps (Schemes 1 and 2). Picolinic acid was refluxed in excess thionyl chloride for 3 h to afford the acyl chloride. The reaction was monitored by ^{1}H NMR spectroscopy in d_6-DMSO, and the disappearance of the carboxylic acid signal at ∼12 ppm indicated complete conversion to the acyl chloride, which was then reacted in situ with 2-, 3-, or 4-aminopyridine

Scheme 1. Synthesis of Ligand Precursors 4−6

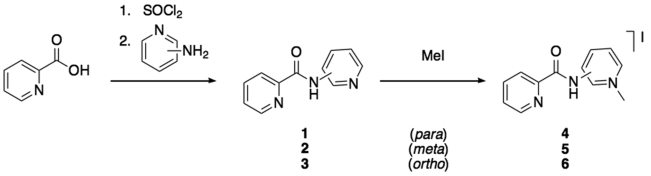

in the presence of NEt_3 to give the amides **1−3** in good yields (∼70%). Formation of the amide precursors was indicated by ^{1}H NMR spectroscopy with the appearance of the low-field NH amide signal in the δ_H 10.4−11 ppm range. Selective methylation of the more nucleophilic amidopyridine nitrogen was achieved by reaction of the amide precursors **1−3** with excess MeI (1.5 equiv), which afforded pyridinium salts **4−6** in good yields (59−89%). Even when a large excess of MeI was used, only the monomethylated pyridinium salts were obtained. The ^{1}H NMR spectra show the appearance of a new singlet at 4.21−4.41 ppm corresponding to the NMe group and a diagnostic deshielding of the aromatic proton signals of the amide-substituted pyridine. In addition, HR-MS indicated a characteristic $[M - I]^+$ ion at 214.0966, 214.0976, and 214.0970 amu for the three salts (theoretical value 214.0980 amu).

While our attempts failed to give the corresponding free ligands by deprotonation of the amide with different bases, metal coordination via in situ deprotonation was successful. Hence, reaction of pyridinium salts **4−6** with the metal precursor [Pd(cod)(Me)Cl] and $AgPF_6$ as halide scavenger in the presence of K_2CO_3 as a base in dry MeCN afforded the cationic Pd(II) complexes **7−9** in good to excellent yields (65−93%, Scheme 2). Coordination of the PYA ligands to the Pd center was confirmed by ^{1}H NMR spectroscopy in CD_2Cl_2, which showed the disappearance of both the NH signal and the cyclooctadiene resonances. Due to the coordination of the PYA ligand, the Pd−Me resonances shift upfield by 0.2−1.1 ppm. Singlets in the 2.16−2.45 ppm range correspond to a coordinated MeCN ligand and corroborate the formation of the cationic solvento complexes. Notably, ^{1}H NMR spectra of complexes **7−9** showed two sets of signals, which are readily distinguished by the different shifts of the singlets attributed to the NMe group (δ_H around 4.2), those of the coordinated MeCN molecule (δ_H around 2.3), and most pronouncedly by the different Pd−Me signal (δ_H between 0 and 1 ppm; Table 1 and Figures S7−S9). The separation of the two signal sets is particularly prominent for complex **9**, for which the palladium-bound Me group features a chemical shift difference $\Delta\delta_H$ of almost 1 ppm. Moreover, the downfield region of the ^{1}H NMR spectra shows a complicated split of the heteroaromatic proton resonances. The two distinct sets of resonances indicate the presence of two species in solution differing in the relative position of the Pd-Me fragment with respect to the two nonequivalent N donors of the chelating pyridyl-PYA ligand (cis/trans isomers). Due to the focus on the PYA and the palladium-bound methyl group, we have termed the complex with the Pd-Me fragment cis to the PYA nitrogen as the cis isomer. NOESY experiments enabled the unambiguous identification of both the cis and the trans isomers of complex **9** (Figure S10). Two different NOEs were observed for the two Pd-Me resonances. The cis isomer showed a NOE interaction between the Pd−Me resonance at δ_H 0.10 and the PYA proton at δ_H 7.72, yet no interaction with any pyridyl hydrogen. In contrast, the Pd−Me resonance at δ_H 1.01 revealed an NOE with the pyridyl proton at δ_H 8.42 and no interference with the PYA protons and was therefore assigned to the trans isomer. Similarly, the cis and trans isomers of **7** and **8** were unequivocally identified. Comparison of the Pd-Me resonance integrals gave the pertinent cis/trans ratio for each of the three complexes. These ratios are remarkably different (Table 1). The trans isomer is predominant in the *p*-PYA complex **7** (cis/trans ratio 1/6), equal to the cis isomer in the *m*-PYA complex

Scheme 2. Synthesis of Palladium Complexes 7–9

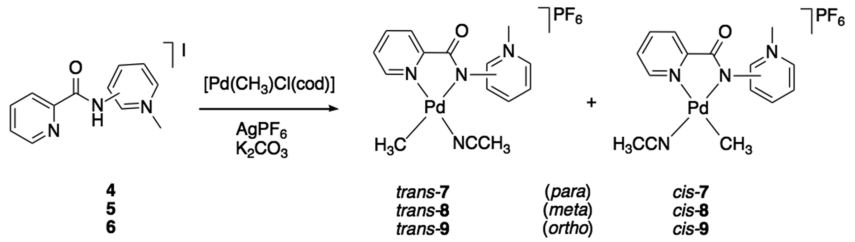

4
5
6

trans-**7**
trans-**8**
trans-**9**

cis-**7**
cis-**8**
cis-**9**

Table 1. Selected ^{1}H NMR Shifts (ppm) in CD_2Cl_2 for Pd-PYA Complexes 7–9

		δ_H(NMe)		δ_H(Pd-NCMe)		δ_H(Pd-Me)	
	cis/trans ratio	cis	trans	cis	trans	cis	trans
7	1/6	4.28	4.28	2.45	2.38	0.48	0.98
8	1/1	4.33	4.35	2.44	2.27	0.32	0.89
9	3/2	4.19	4.24	2.45	2.16	0.10	1.01

8 (1/1 ratio), while complex **9** favors the cis isomer (3/2 cis/trans ratio).

The notable difference in cis/trans ratio is attributed to the different donor properties of the three isomeric PYA units, since the position of the NMe group in the pyridylidene ring has a direct effect on the donor ability of the amide and on its electronic flexibility. Accordingly, *p*-PYA ligands are highly flexible and, depending on several factors such as the electron density at the coordinated metal center or the solvent polarity, they undergo valence isomerism between a zwitterionic, π-basic form with an anionic X-type amido ligand and a charge-balancing remote pyridinium unit and a neutral π-acid L-type imine resonance form (Figure 2). In contrast, *m*-PYA ligands

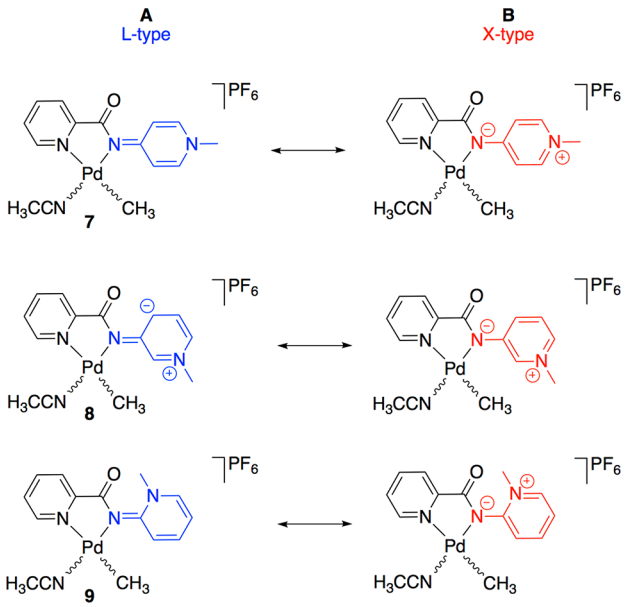

Figure 2. Resonance structures of Pd(II)-PYA complexes **7**–**9**.

have a strongly dipolar, presumably mesoionic form[10e,11] and no neutral resonance structure can be drawn. This situation increases the X-type character and therefore the overall ligand donor strength. For *o*-PYAs, both zwitterionic and neutral resonance structures can be drawn as for *p*-PYAs; however, steric constraints between the N_{PYA}–Me group and the amide C═O force the pyridylidene heterocycle to rotate out of the amide plane. This dihedral twist minimizes any conjugation through the exocyclic C_{PYA}–N_{PYA} bond and increases the relevance of the zwitterionic amide resonance structure and an X-type metal coordination.[12] Hence, the contribution of the neutral imine form is negligible in comparison to *p*-PYA. These considerations place the *m*- and *o*-PYA ligands in a different donor category than the *p*-PYA ligand, and this difference is also reflected in the diverging stability of the cis isomers.

Related studies with nonsymmetric N^N′-chelating α-diimine ligands having an acenaphthene (ArBIAN),[13] 1,4-diaza-2,3-butadiene (ArDAB),[14] or iminopyridine skeleton[15] revealed that the position of the palladium-bound methyl group is mainly dictated by the electronic properties of the trans-positioned ligand, and strong donors direct the methyl group to a mutual cis position. According to this model, the large predominance of *trans*-**7** over the cis isomer (6/1 ratio) indicates only weak donor properties of the *p*-PYA ligand, which is rationalized by the neutral π-acidic and hence less electron donating imine-type resonance form of the PYA ligand in CH_2Cl_2. In contrast, the ratio of the cis isomer in complexes **8** and **9** is much larger (1/1 and 3/2 cis/trans ratio), indicative of markedly stronger donor properties of the *m*- and *o*-PYA ligands, which is in agreement with the electronic and steric effects that lead to an enhanced X-type and π-basic character of the ligand. Variable-temperature ^{1}H NMR analysis of complex **9** in the 25–75 °C range did not show any significant broadening of the signals that would hint to fluxional behavior and a potential cis/trans isomerization process on the NMR time scale.

Single crystals of complex **7** suitable for X-ray diffraction analysis were obtained by slow diffusion of *n*-pentane into a CH_2Cl_2 solution. The asymmetric unit of this crystal only contained the trans isomer, which is also the major species in solution. The palladium center in *trans*-**7** has a slightly distorted square planar geometry with the N^N′-chelating pyridyl-PYA ligand, a Me group in a position trans to the PYA nitrogen, and a molecule of acetonitrile occupying the fourth coordination site (Figure 3). The bond lengths and angles around the palladium center are within expectation for Pd(II) complexes containing N^N′-bidentate ligands.[15a] As observed in related iridium and ruthenium complexes,[10a–d] the C–C bond lengths in the pyridylidene ring suggest a pronounced diene-type form, in which the C_α–C_β bond lengths (C11–C12 = 1.369(6) Å and C8–C9 = 1.367(6) Å) are considerably shorter than the C_β–C_γ bond distances (C11–C7 = 1.425(6) Å and C7–C8 = 1.405(6) Å, respectively). The pyridylidene ring is slightly twisted out of the palladium coordination plane, as indicated by the Pd–N_{PYA}–C_γ–C_β torsion angle of 28.2°. This angle is smaller in comparison to the 35–45° observed in PYA-iridium complexes and points to a stronger contribution of the neutral π-acidic imine form of the ligand,[10d] presumably

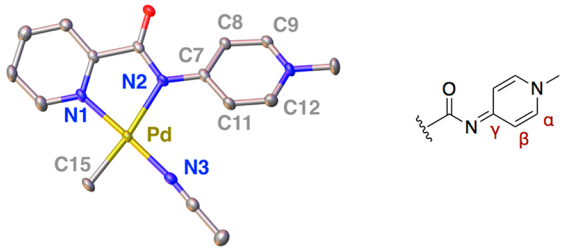

Figure 3. Crystal structure of complex *trans*-**7**. Selected bond lengths (Å) and angles (deg): Pd–N1 2.030(4), Pd–N2 2.174(3), Pd–C15 2.032(4), Pd–N3 1.998(4), N2–C7 1.376(6), C7–C8 = 1.405(6), C7–C11 = 1.425(6), C8–C9 = 1.367(6), C11–C12 = 1.369(6); N1–Pd–N2 80.17(14), N1–Pd–C15 84.48(18), C15–Pd–N3 93.13(17), N2–Pd–N3 102.22(15).

as a consequence of the higher electron density and ensuing higher propensity for π back-bonding of palladium(II) in comparison to iridium(III) or ruthenium(II). In agreement with this notion, the exocylic C_γ–N_{PYA} bond is remarkably shorter than classical C–N single bonds (N2–C7 = 1.376(6) Å, cf. N_{py}–C_{Me} = 1.475(6) Å), suggesting considerable double-bond imine contribution.

Complexes **7**–**9** were further analyzed in different solvents in order to gain more insights into the electronic adaptiveness of the ligand and how this flexibility affects the cis/trans ratio. ^{1}H NMR spectra of complexes **7**–**9** in d_6-DMSO featured a singlet at 2.07 ppm corresponding to free MeCN. Elimination of MeCN indicates ligand exchange from MeCN to DMSO[10c] and formation of the solvento complexes **10**–**12** (Scheme 3).

Scheme 3. Formation of the DMSO Pd(II)-PYA Complexes 10–12

7 (*para*) **10**
8 (*meta*) **11**
9 (*ortho*) **12**

Moreover, only one Pd–Me resonance was observed for each complex by ^{1}H NMR spectroscopy, which indicates the presence of only one isomer (Figures S11–S16). The NOE of the Pd–Me singlet at δ_H 0.17 ppm with the C_{PYA}H hydrogen at δ_H 7.75 ppm but not with any C_{pyr}H identifies the product as *cis*-**10** exclusively.[16] The prevalence of the cis isomer is in agreement with the hypothesis that the more π basic zwitterionic PYA form is predominant in polar solvents, which increases the donor strength of the ligand and hence favors the cis arrangement of the palladium-bound methyl group. Closer inspection of the Pd–Me resonance frequency showed a correlation between its chemical shift and the PYA donor properties, in agreement with the hypothesis that this signal is an excellent probe for assessing the electron donor properties of the ligands around the metal center.[15a] Thus, the most electron donating *o*-PYA ligand (complex **12**) featured the Pd–Me resonance more upfield (δ_H −0.12 ppm) than the less electron donating *p*-PYA (δ_H 0.17 ppm in **10**). Palladium complex **11** with the *m*-PYA ligand is intermediate (δ_H 0.05 ppm). This trend is supported by the chemical shift differences of the Pd–Me resonance of complexes *cis*-**7**–**9** in CD_2Cl_2 (vide supra).

Analogous studies in CD_3CN also showed the disappearance of the Pd–NCMe signal, indicating exchange of MeCN by the deuterated analogue. In deuterated MeCN, two sets of signals were observed, indicating a cis/trans mixture as detected in CD_2Cl_2. However, the cis/trans ratios in CD_3CN are shifted toward the cis isomer in comparison to the measurements in CD_2Cl_2. In deuterated MeCN, the ratios are 1/2 (rather than 1/6 in CD_2Cl_2) for **7**, 3/1 (instead of 1/1) for **8**, and 5/1 (vs 3/2) for complex **9**. This significant increase in the cis isomer is attributed to the stronger donor properties of the PYA ligand due to the larger contribution of the zwitterionic resonance form in polar solvents and underlines the electronic flexibility and adaptiveness of the PYA ligand. The increase of the cis complex relative to the trans isomer correlates with the increased solvent polarity (ε_{CD2Cl2} = 9.08; ε_{CD3CN} = 37.5; ε_{DMSO} = 46.7)[17] and is therefore presumably linked to the increasing contribution of the zwitterionic amide form of the PYA ligand. This trend is amplified by the weaker trans influence of DMSO[10c,13,14,18] in comparison to MeCN, which increases the difference between the Me and the solvent ligand. These two superimposed effects (larger zwitterionic electron-donating form of PYA ligand plus weak trans influence of DMSO) rationalize the absence of detectable amounts of the trans isomer for complexes **10**–**12**.

Reactivity and Catalysis. The insertion of ethylene into a metal–alkyl bond represents a key step in the metal-catalyzed single-site homo- and copolymerization of alkenes. Complexes **7**–**9** comprise a weakly bound solvent molecule for substitution by the alkene, a Pd–Me fragment for subsequent insertion, and a dissymmetric N^N′-ligand scaffold that should alter the affinity of the metal to bind to monomers. Therefore, these complexes were tested in ethylene/methyl acrylate copolymerization in 2,2,2-trifluoroethanol (TFE) under standard conditions.[13,14] Analysis of the products by ^{1}H NMR spectroscopy showed the formation of ester species that were not attributed to free methyl acrylate. Analysis by GC-MS confirmed the presence of butenes and methyl pentenoates, indicating that complexes **7**–**9** are ineffective in polymerization yet are able to incorporate acrylate in the olefin coupling process. Quantitative GC-MS analysis (Scheme 4) reveals two key effects. First, the activity increases with increasing steric congestion, revealing almost identical productivity for the *m*-PYA complex **8** and the para analogue **7** ([butenes + pentenoates] = 45 ± 2 mM for 1 mM palladium complex, corresponding to a TON close to 45), yet considerably better

Scheme 4. Olefin Dimerization Catalyzed by Pd(II)-PYA Complexes 7–9 Producing a Mixture of Ethylene Homodimer and Ethylene/Methyl Acrylate (MA) Heterodimer[a]

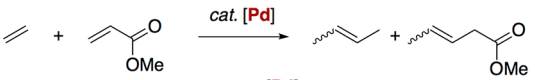

[Pd]			MA/C_2H_4
7	36.0	7.8	17.8%
8	31.0	14.8	32.3%
9	113.3	40.1	26.1%

[a]Quantities of homodimer (second column) and ethylene/MA heterodoxer (third column) in mM according to GC-MS analysis; 1 mM palladium complex; far right column: ratio for the insertion of the second olefin into the Pd–Et intermediate (see text).

performance of the *o*-PYA complex **9** (TON ≈ 153). Second, the distinct donor properties of the PYA system induce a remarkably high incorporation of methyl acrylate (18−32% for the second olefin insertion step). This is one of the highest ratios of methyl acrylate insertion with N^N-type ligands known to date,[18] though higher incorporation of polar monomers has been achieved with P^O-bidentate ligands.[19] We note that the affinity for acrylate insertion is directly correlated to the donor properties of the PYA unit and is highest for complexes **8** and **9**, which contain a PYA with a pronouncedly anionic N-donor character (see above). These stronger donor properties favor the coordination of a π-acidic olefin, thus rationalizing the better incorporation of methyl acrylate by complexes **8** and **9** in comparison to the less electron rich palladium center in complex **7**.

Mechanistic studies were carried out in order to identify the role of the Pd-PYA complexes in the olefin dimerization process. The reactivity of complexes **7**−**9** with ethylene was investigated by in situ NMR experiments performed by saturating a 10 mM CD_2Cl_2 solution of each complex with ethylene at room temperature. Monitoring the reaction over time revealed different rates of ethylene consumption for all three palladium catalysts. While complex **7** only reaches 50% conversion of ethylene in 2 h together with formation of Pd black (see below), complexes **8** and **9** achieve essentially full conversion within 60 and 30 min, respectively (Figure 4 and

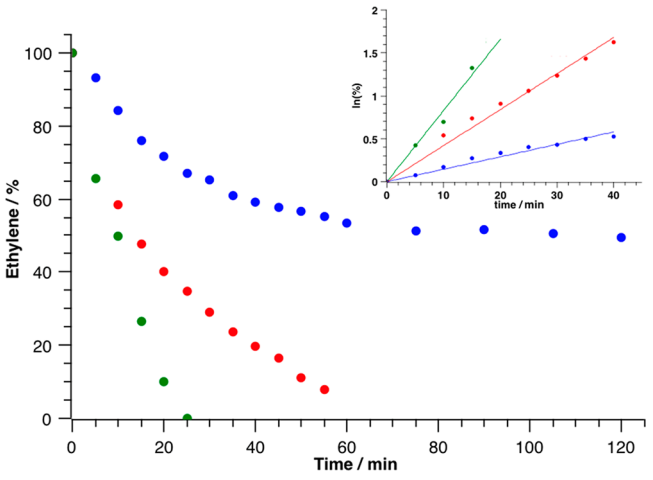

Figure 4. Ethylene consumption using complexes **7** (blue), **8** (red), and **9** (green) (10 mM solution of palladium complex in CD_2Cl_2 saturated with ethylene): consumption of ethylene measured by ^{1}H NMR spectroscopy (δ_H 5.31) relative to MeCN as internal standard. The inset shows the corresponding ln(%) vs time at initial times, with k_{rel} values of 0.19, 0.50, and 1 and R^2 values of 0.964, 0.961, and 0.974, respectively, for complexes **7**−**9**.

Figure S20). Further analyses of initial rates for ethylene conversion were performed by assuming a first-order rate law. A logarithmic plot of the change in substrate concentration vs time indeed produced a linear fit for the conversions achieved with complexes **7**−**9** (inset Figure 4). When the initial rates are considered, complex **7** shows the lowest activity, while complex **8** is about 2.5 times more active and complex **9** about 5 times more active than complex **7**. This trend in activity is in agreement with the cis/trans ratio of the complexes: palladium complex **9** with a cis/trans ratio of 1.5 shows greater activity than complexes **8** and **7** (cis/trans ratio of 1 and 0.16). These correlations suggest that the catalytic activity is dictated by the donor properties of the PYA unit.

Analysis of the ^{1}H NMR spectra recorded 5 min after saturation with ethylene shows that the signals corresponding to the palladium precursors **7**−**9** disappeared, indicating that all complexes (both cis and trans isomers) are converted into new species. In the aliphatic region of the ^{1}H NMR spectrum different signals corresponding to free MeCN, propene, and butenes are present together with a triplet at 0.99 ppm and a quartet at 2.05 ppm (same chemical shift values for the products of all three complexes **7**−**9**; Figures S17−S19), which were attributed to a palladium-bound ethyl group.[20,21] In addition, a second Pd-ethyl fragment was detectable in the reactions of ethylene with complexes **7** and **8**, though the signals were not well-resolved in the former and were only observed indirectly through NOESY experiments at low temperature. In both complexes, the sum of the integrals of the Pd-ethyl fragments reveals stoichiometric ratios of the Pd−Et species and free MeCN, demonstrating quantitative formation of the ethyl species as the catalytic resting state.[20,21] For complex **9**, the reaction was too fast to allow for any characterization of the Pd-ethyl species, and a sample after 5 min revealed only about 25% of the Pd-ethyl species. Low-temperature 2D NMR experiments for the species derived from complex **8** provided further insights. Experiments were performed at −30 °C, which essentially stalls further catalytic reactions. Through a NOESY experiment, the set of signals at lower frequency (δ_H 0.53 and 1.07) revealed a correlation with the PYA protons and was therefore assigned to the cis isomer, while the less shielded ethyl group (δ_H 0.99 and 2.05) was assigned to the trans isomer (Figure S21). Analysis of the intermediates derived from complex **7** and ethylene corroborate this assignment, revealing a correlation between the PYA proton resonances and a set of signals at lower frequency (δ_H 0.80 and 1.20), which was therefore assigned to the cis isomer (Figure S22). As a consequence, the Pd-ethyl species that is present at room temperature upon reaction of ethylene with any of the three complexes is the trans isomer.

Evaluation of the Pd−Et resonances from room-temperature catalytic experiments with complex **8** reveals a gradual depletion of the cis isomer with a concomitant increase in the concentration of the trans isomer (Figure 5). The isomerization process follows first-order kinetics (inset Figure 5). While such isomerization has been known for palladium-methyl complexes with P^O-type ligands (i.e., the catalyst precursor) and has been predicted by computation to occur also in the Pd−Et intermediate,[22] this is the first identification of this process experimentally. This observable isomerization emphasizes the distinct differences in the two nitrogen donor sites in the pyridyl-PYA system when the zwitterionic polar structure is enforced as in complex **8**, in combination with the stronger trans effect of ethylene compared to the ethyl ligand. In addition, these data suggest a different reactivity of *cis* and *trans* Pd-ethyl isomers, which can be considered as the real active species and the resting state of the catalytic cycle, respectively. The rate of the catalytic olefin dimerization correlates well with the isomeric distribution in the different precursors, when it is considered that for the Pd−Me precursor the cis/trans isomerization is not evident on the NMR time scale at room temperature and when similar thermodynamic stabilities for the Pd−Me and the Pd−Et species are assumed. Hence, complex **9** has the highest Pd−Me cis/trans ratio, produces the fastest catalyst, and reveals only a small fraction

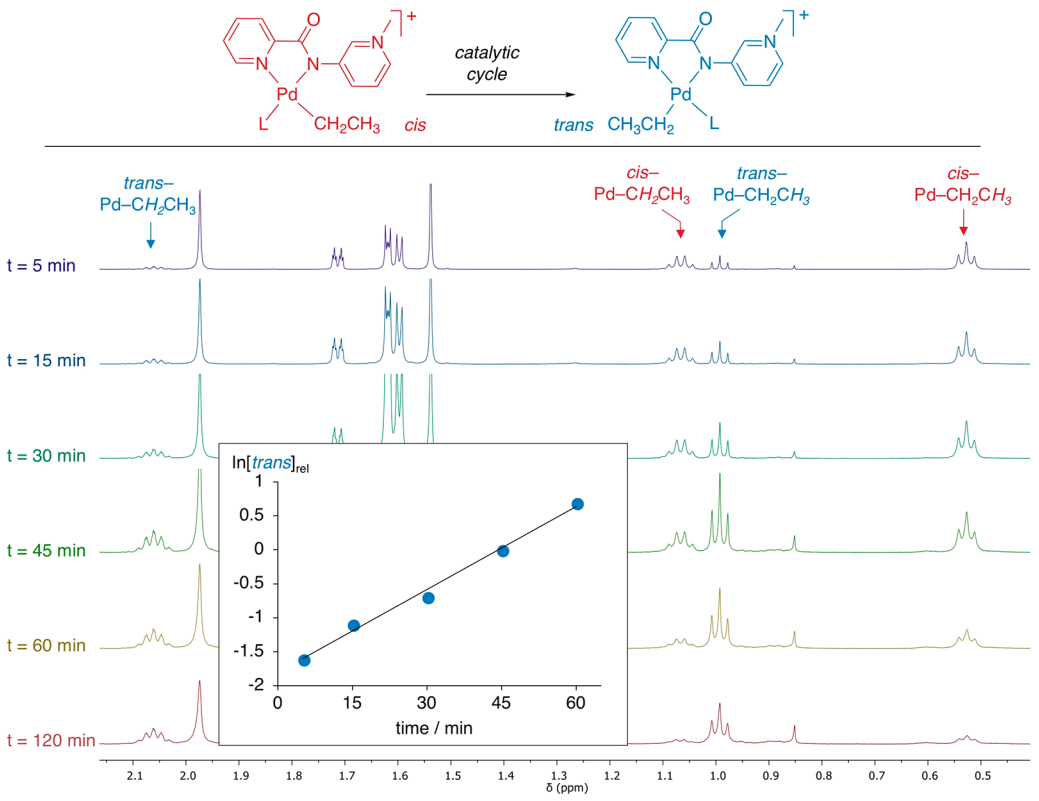

Figure 5. Stacked ^{1}H NMR spectra of complex **8** in the presence of ethylene, revealing the gradual isomerization of the *cis*-Pd–ethyl isomer into the trans species. The inset shows a first-order fit of the time-dependent concentration change (correlation R^2 = 0.992, in CD_2Cl_2 at 298 K).

of the trans Pd-ethyl isomer in the resting state. Complex **8** exhibits no preference for the cis or trans isomer and exhibits intermediate catalytic activity, and both Pd–Et isomers were detected at room temperature in time-dependent ratios. Finally complex **7** favors the trans Pd–Me isomer and shows the slowest ethylene conversion, and only minor quantities of the *cis*-Pd–Et isomer were detected and the *trans*-Pd–ethyl species was predominant as the catalyst resting state.

On the basis of these NMR data, a mechanism for the catalytic ethylene conversion emerges (Scheme 5). The observation of propene indicates substitution of the coordinated MeCN by ethylene, followed by migratory insertion into the Pd–Me bond and β-hydride elimination to form propene.[3,20,22h,23] Reaction of the resulting palladium hydride species with a molecule of ethylene then leads to the formation of the Pd–ethyl species as the resting state (cf. NMR spectra).[3,20] Migratory insertion of ethylene into the *cis*-Pd–Et species is the rate-limiting step at high ethylene concentration. As the reaction progresses, this rate-limiting step shifts toward the isomerization of the dormant *trans*-Pd–Et complex to its cis isomer.

A second ethylene insertion followed by β-hydride elimination provides a pathway for the formation of butene (Scheme 5). Detailed analysis by NMR spectroscopy shows the presence of only 2-butenes as a result of a fast chain-walking process from the terminal to the internal position prior to product dissociation via β-hydride elimination.[3] The absence of any 1-butene or higher olefin in the product mixture indicates that β-H elimination from the Pd–butyl intermediate and olefin isomerization are both much faster processes than insertion of a third ethylene monomer. Monitoring of the reaction over a prolonged time did not show any formation of higher oligomers or polymers, suggesting that the active palladium species does not react with internal alkenes.

The solution of palladium complex **7** in CD_2Cl_2 produced significant quantities of Pd black already after 2 h under catalytically relevant conditions in a NMR setup (50% conversion). In contrast, Pd black was only observed after full ethylene consumption when complexes **8** and **9** were used as precatalysts, which may be attributed to the specific conditions of these NMR experiments with limited availability of ethylene. These observations indicate that for complex **7** the cessation of catalytic activity after 2 h is due to catalyst decomposition, in agreement with the low donor capability of the *p*-PYA ligand as evidenced by the NMR analysis. For the ligands under investigation their donor properties are related to the zwitterionic amido character vs the neutral imine-type resonance form. Tentatively, the catalyst lifetime might be also related to these parameters: catalysts derived from complexes **8** and **9** are stabilized by the more zwitterionic amido character of the ligands, whereas the catalytic species derived from complex **7** is less stable due to the significant contribution of the neutral imine-type resonance form.

In agreement with such a model, catalytic runs with complexes **7**–**9** in 2,2,2-trifluoroethanol as a more polar solvent ($\varepsilon_{CF3CH2OH}$ = 26.7)[24] did not lead to any detectable formation of Pd black in the first 2 h of reaction. These observations corroborate the notion that CF_3CH_2OH stabilizes the Pd-hydride,[25] while less polar solvents such as CH_2Cl_2 impart less stability.

Due to the specific reactivity of Pd-PYA complexes **7**–**9** toward the dimerization of ethylene, we were interested to see whether higher olefins were dimerized as well. Therefore, the

Scheme 5. Proposed Mechanism for Catalyst Activation, Ethylene Dimerization[a]

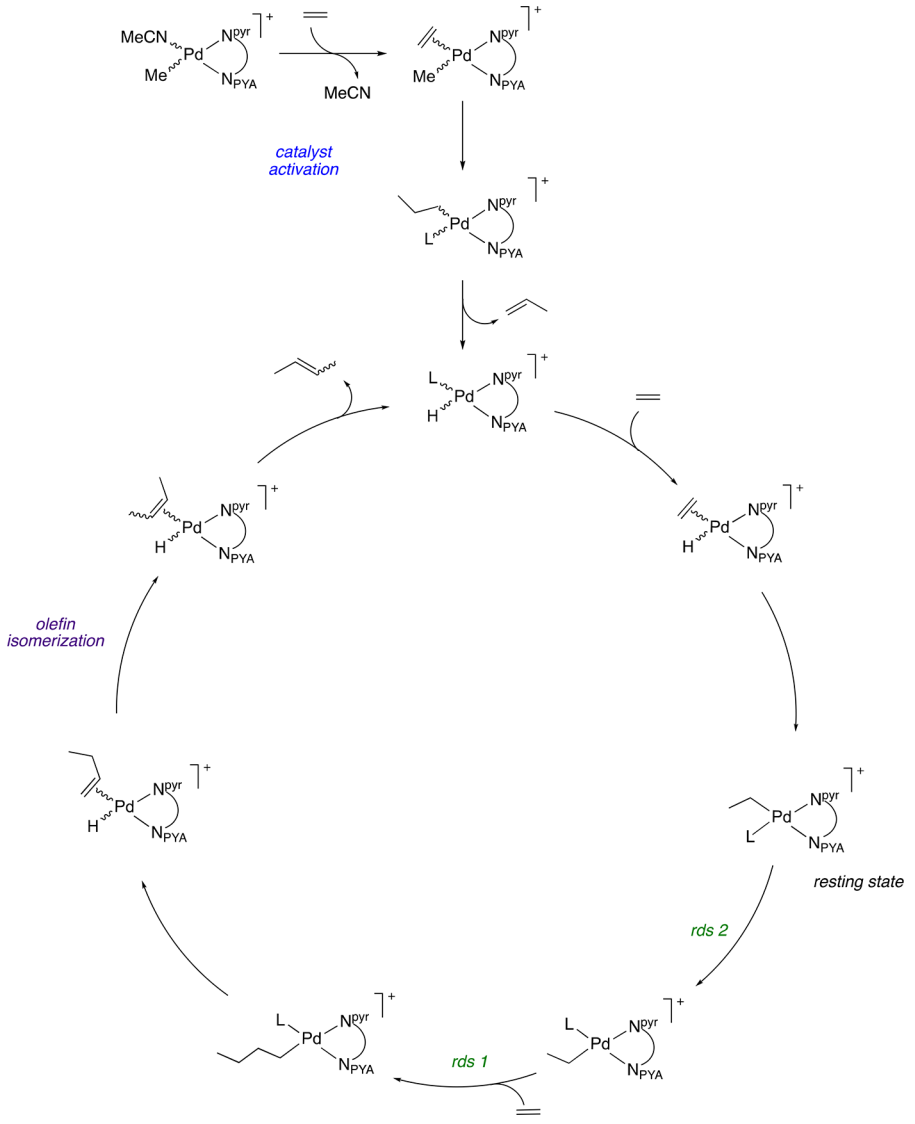

[a]L is either an olefin, agostic stabilization, or weak solvent interactions. rds 1 denotes migratory insertion of ethylene into the Pd−Et bond as the rate-limiting step (for complexes **8** and **9** in the presence of large excess of ethylene), and rds 2 denotes the trans−cis isomerization as the rate-limiting step when ethylene availability is limited, and for complex **7**, which favors the trans isomer.

most active complex **9** was tested as a precatalyst for the dimerization of 1-hexene in CH_2Cl_2 solution at 30 °C. After 18 h, only 10% conversion was achieved when a 0.01 mol % catalyst loading was used. Conversion increased to 80% when the catalyst loading was increased to 0.1 mol % (18 h) and reached full conversion within 2 h when 10 mol % catalyst loading was used. Analysis of the product mixture by ^{1}H NMR spectroscopy and GC-MS showed the presence of unreacted 1-hexene (at lower catalyst loadings of 0.01 and 0.1 mol %) and in particular the formation of internal hexenes and internal heptenes as products (9/1 hexene/heptene ratio at 10 mol % catalyst; Scheme 6 and Figures S23−S25). Olefin isomerization has ample precedent.[26] Formation of heptene is again the result of the substitution of the coordinated MeCN ligand by 1-hexene, followed by insertion into the Pd−Me bond and subsequent β-hydrogen elimination. Hence, coordination of 1-hexene to the palladium center is not prevented. However, once the hydride is formed, coordination of 1-hexene only results in isomerization, not in coordination/insertion of a

Scheme 6. 1-Hexene Isomerization using Pd-PYA Complex 9

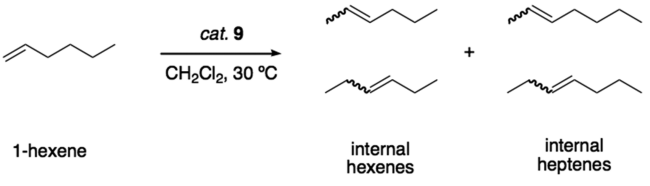

second equivalent of 1-hexene. Accordingly, chain walking at these PYA palladium complexes is a comparatively fast process, and the rate of β-hydrogen elimination from the intermediate palladium-hexyl species is substantially faster than the coordination or insertion of another olefin molecule into the Pd−R bond. These rate differences prevent polymerization and induce fast isomerization as observed for butene, hexene, and heptene. A refined ligand design involving the introduction of sterically shielding substituents into the pyr-PYA ligand

scaffold might provide a methodology for tailoring these relative rates and for enhancing insertion over chain walking and therefore for inducing polymerization.

CONCLUSIONS

New pyridine-functionalized pyridylidene amide palladium complexes were synthesized as catalyst precursors for the conversion of olefins. Modification of the donor properties of the PYA by changing the position of the amide unit allows the activity of the palladium center to be tailored. A clear relationship between the ligand electronic properties and the activity of catalytic ethylene conversion was demonstrated. Thus, complexes with less electron donating *p*-PYA ligands showed lower catalytic activity than palladium complexes bearing more electron donating ligands such as *m*- and *o*-PYA. Mechanistic NMR investigations provided for the first time direct evidence for *cis* and *trans*-Pd-ethyl intermediates—one as the active species and the other as the resting state of the catalytic cycle—and for a swap of the rate-determining step from ethylene migratory insertion to the trans/cis isomerization of this intermediate, depending on the ethylene concentration in solution. Selective dimerization of ethylene was observed, followed by an isomerization process of the terminal to internal alkenes through a fast chain walking process, which prevents further polymerization. When methyl acrylate is used as a polar comonomer, this monomer is inserted in high percentage, in particular with strongly donating *m*- and *o*-PYA units in the ligand structure. Due to this high methyl acrylate conversion, further work is being directed toward modification of the isomerization vs insertion kinetics, which may be achieved by introducing sterically more demanding substituents on these synthetically versatile ligands.

EXPERIMENTAL SECTION

General Considerations. The metal precursor [Pd(cod)(Me)Cl][27] and ligand precursor **1**[9d] were synthesized as reported in the literature. An optimized synthetic procedure was followed to prepare compounds **2** and **3**. Analytical data of these compounds are in agreement with those reported.[9d,28] Dry solvents for reactions were filtered over columns of dried neutral aluminum oxide under a positive pressure of argon. All other reagents were used as received from commercial suppliers. Unless specified, NMR spectra were recorded at 25 °C on Bruker spectrometers operating at 300 or 400 MHz (^{1}H NMR) and 100 MHz (^{13}C NMR), respectively. Chemical shifts (δ in ppm, coupling constants J in Hz) were referenced to residual solvent signals (^{1}H, ^{13}C). Assignments are based on homo- and heteronuclear shift correlation spectroscopy. Purity of bulk samples of the complexes has been established by NMR spectroscopy, and by elemental analysis, which were performed by the University of Bern Microanalytic Laboratory using a Thermo Scientific Flash 2000 CHNS-O elemental analyzer. Residual solvent was confirmed by NMR spectroscopy. High-resolution mass spectrometry was carried out with a Thermo Scientific LTQ Orbitrap XL (ESI-TOF). The purity of the new compounds **7**–**9** was established by ^{13}C NMR spectroscopy combined with either HR-MS or elemental analyses (Supporting Information).

General Procedure for the Formation of Amides 2 and 3. Picolinic acid (1.231 g, 10 mmol) was refluxed in $SOCl_2$ (10 mL, 0.14 mol) for 3 h under an N_2 atmosphere. The excess of $SOCl_2$ was removed under reduced pressure in a well-ventilated fumehood. The residue was dissolved in dry THF (40 mL) and transferred via cannula to a solution of the corresponding aminopyridine (0.940 g, 10 mmol) in THF (50 mL) with the presence of NEt_3 (2.5 mL, 18 mmol). The mixture was refluxed for 48 h, filtered, and the solvent was removed under reduced pressure. The brown solid residue was purified by column chromatography (SiO_2) to yield the pure products as white solids.

General Procedure for the Synthesis of Pyridinium Salts 4–6. Compounds **1**–**3** (398 mg, 2.0 mmol) were dissolved in MeCN (15 mL) in a pressure tube. MeI (187 μL, 3.0 mmol) was added, and the reaction mixture was stirred for 18 h at 80 °C. The solution was cooled to room temperature and concentrated to 5 mL. Et_2O (50 mL) was added, and the formed yellow precipitate was filtered and washed with cold Et_2O to yield **4**–**6** as yellow solids.

Compound 4. Compound **4** was prepared according to the general procedure from **1**. Yield: 607 mg, 89%. ^{1}H NMR (300 MHz, d_6-DMSO): δ 12.00 (s, 1H, NH), 8.85–8.80 (m, 1H, CH_{pyr}), 8.81 (d, $^3J_{HH}$ = 7.1 Hz, 2H, CH_{PYA}), 8.49 (d, $^3J_{HH}$ = 7.1 Hz, 2H, CH_{PYA}), 8.23 (d, $^3J_{HH}$ = 7.8 Hz, 1H, CH_{pyr}), 8.15 (td, $^3J_{HH}$ = 8.8, $^4J_{HH}$ = 1.7 Hz, 1H, CH_{pyr}), 7.80 (ddd, $^3J_{HH}$ = 7.8, 4.7, $^4J_{HH}$ = 1.3 Hz, 1H, CH_{pyr}), 4.21 (s, 3H, NCH_3). ^{13}C{^{1}H} NMR (100 MHz, d_6-DMSO): δ 164.7 (CO), 151.4 (C_{pyr}), 148.8 (CH_{pyr}), 148.2 (C_{pyr}), 145.9 (CH_{PYA}), 138.5 (CH_{pyr}), 128.2 (CH_{pyr}), 123.5 (CH_{pyr}), 115.8 (CH_{PYA}), 46.5 (NCH_3). HR-MS: m/z calculated for $C_{12}H_{12}N_3O$ $[M-I]^+$, 214.0980; found, 214.0966. Anal. Calcd for $C_{12}H_{12}IN_3O$: C, 42.25; H, 3.55; N, 12.32. Found: C, 41.97; H, 3.87; N, 12.47.

Compound 5. Compound **5** was prepared according to the general procedure from **2**. Yield: 512 mg, 75%. ^{1}H NMR (300 MHz, d_6-DMSO): δ 11.69 (s, 1H, NH), 9.63 (s, 1H, CH_{pyr}), 8.89 (d, $^3J_{HH}$ = 8.8 Hz, 1H, CH_{PYA}), 8.82 (dt, $^3J_{HH}$ = 4.6, $^4J_{HH}$ = 1.4 Hz, 1H, CH_{pyr}), 8.76 (d, $^3J_{HH}$ = 5.9 Hz, 1H, CH_{PYA}), 8.22 (dt, $^3J_{HH}$ = 7.9, $^4J_{HH}$ = 1.4 Hz, 1H, CH_{pyr}), 8.18–8.10 (m, 2H, CH_{PYA} + CH_{pyr}), 7.78 (ddd, $^3J_{HH}$ = 7.8, 4.6, $^4J_{HH}$ = 1.2 Hz, 1H, CH_{pyr}), 4.41 (s, 3H, NCH_3). ^{13}C{^{1}H} NMR (100 MHz, d_6-DMSO): δ 163.8 (CO), 148.8 (CH_{pyr}), 148.3 (C_{pyr}), 140.4 (CH_{PYA}), 138.5 (CH_{PYA}), 138.4 (C_{PYA}), 136.7 (CH_{PYA}), 135.0 (CH_{PYA}), 127.9 (CH_{pyr}), 127.1 (CH_{pyr}), 123.1 (CH_{pyr}), 48.6 (NCH_3). HR-MS: m/z calculated for $C_{12}H_{12}N_3O$ $[M-I]^+$, 214.0980; found, 214.0976. Anal. Calcd for $C_{12}H_{12}IN_3O$: C, 42.25; H, 3.55; N, 12.32. Found: C, 42.53; H, 3.77; N, 12.67.

Compound 6. Compound **6** was prepared according to the general procedure from **3**. Yield: 402 mg, 59%. ^{1}H NMR (300 MHz, d_6-DMSO): δ 11.67 (s, 1H, NH), 8.97 (dd, $^3J_{HH}$ = 6.4, $^4J_{HH}$ = 1.6 Hz, 1H, CH_{PYA}), 8.85 (dt, $^3J_{HH}$ = 4.7, $^4J_{HH}$ = 1.4 Hz, 1H, CH_{pyr}), 8.61 (ddd, $^3J_{HH}$ = 9.0, 7.7, $^4J_{HH}$ = 1.7 Hz, 1H, CH_{PYA}), 8.46 (dd, $^3J_{HH}$ = 8.5, $^4J_{HH}$ = 1.4 Hz, 1H, CH_{PYA}), 8.29 (dt, $^3J_{HH}$ = 7.9, $^4J_{HH}$ = 1.4 Hz, 1H, CH_{pyr}), 8.21 (td, $^3J_{HH}$ = 7.7, $^4J_{HH}$ = 1.7 Hz, 1H, CH_{pyr}), 7.91–7.82 (m, 2H, CH_{pyr} + CH_{PYA}), 4.34 (s, 3H, NCH_3). ^{13}C{^{1}H} NMR (100 MHz, d_6-DMSO): δ 162.8 (CO), 148.6 (CH_{pyr}), 147.5 (C_{pyr}), 147.3 (C_{PYA}), 146.2 (CH_{PYA}), 145.3 (CH_{PYA}), 139.1 (CH_{pyr}), 128.5 (CH_{pyr}), 123.4 (CH_{pyr}), 122.9 (CH_{PYA}), 122.8 (CH_{PYA}), 43.9 (NCH_3). HR-MS: m/z calculated for $C_{12}H_{12}N_3O$ $[M-I]^+$, 214.0980; found, 214.0970. Anal. Calcd for $C_{12}H_{12}IN_3O$: C, 42.25; H, 3.55; N, 12.32. Found: C, 42.61; H, 3.73; N, 12.62.

General Procedure for the Synthesis of Palladium Complexes 7–9. Compounds **4**–**6** (86 mg, 0.25 mmol), [Pd(cod)(Me)Cl] (79 mg, 0.30 mmol), $AgPF_6$ (126 mg, 0.5 mmol), and K_2CO_3 (69 mg, 0.50 mmol) were stirred in dry MeCN (10 mL) under N_2 atmosphere for 3 h. The volatiles were removed under reduced pressure, and dry CH_2Cl_2 (20 mL) was added. The mixture was filtered through a short pad of Celite and washed with more CH_2Cl_2 (20 mL). All filtrates were combined and evaporated to dryness to obtain Pd complexes **7**–**9** as pale yellow solids. The crude product was purified by recrystallization from CH_2Cl_2/pentane.

Compound 7. Compound **7** was prepared according to the general procedure from **4**. Yield: 121 mg, 93%. HR-MS: m/z calculated for $C_{15}H_{17}N_4OPd$ $[M-PF_6]^+$, 375.0437; found, 375.0415. Spectroscopic data for the trans isomer are as follows. ^{1}H NMR (300 MHz, CD_2Cl_2): δ 8.43 (d, $^3J_{HH}$ = 5.4 Hz, 1H, CH_{pyr}), 8.25 (d,$^3J_{HH}$ = 7.5 Hz, 1H, CH_{pyr}), 8.12 (d, $^3J_{HH}$ = 7.1 Hz, 2H, CH_{PYA}), 8.07 (ddd, $^3J_{HH}$ = 7.5, 5.6, $^4J_{HH}$ = 1.6 Hz, 1H, CH_{pyr}), 7.97 (d, $^3J_{HH}$ = 7.1 Hz, 2H, CH_{PYA}), 7.58 (ddd, $^3J_{HH}$ = 7.5, 5.6, $^4J_{HH}$ = 1.6 Hz,, 1H, CH_{pyr}), 4.28 (s, 3H, NCH_3), 2.38 (s, 3H, Pd–$NCCH_3$), 0.98 (s, 3H, Pd–CH_3). ^{13}C{^{1}H} NMR (100 MHz, CD_2Cl_2): δ 145.8 (CH_{pyr}), 140.5 (CH_{PYA}), 127.6 (CH_{pyr}), 127.3 (CH_{PYA}), 47.0 (NCH_3), 2.0 (Pd–CH_3). Spectroscopic data for the cis isomer are as follows; only the

aliphatic region could be assigned. ^{1}H NMR (300 MHz, CD_2Cl_2): δ 4.28 (s, 3H, NCH_3), 2.45 (s, 3H, Pd−$NCCH_3$), 0.48 (s, 3H, Pd−CH_3).

Compound ***8***. Compound **8** was prepared according to the general procedure from **5**. Yield: 92 mg, 71%. HR-MS: m/z calculated for $C_{15}H_{17}N_4OPd$ $[M - PF_6]^+$, 375.0437; found, 375.0412. Anal. Calcd for $C_{15}H_{17}F_6N_4OPPd{\cdot}0.25CH_2Cl_2$: C, 33.80; H, 3.25; N, 10.34. Found: C, 34.25; H, 3.39; N, 9.95. Spectroscopic data for the trans isomer are as follows. ^{1}H NMR (300 MHz, CD_2Cl_2): δ 8.55 (s, 1H, CH_{PYA}), 8.42−8.39 (m, 1H, CH_{pyr}), 8.24−8.19 (m, 2H, CH_{pyr} + CH_{PYA}), 8.17−8.12 (m, 1H, CH_{PYA}), 8.07 (t, $^3J_{HH}$ = 7.7, Hz, 1H, CH_{pyr}), 7.87 (dd, $^3J_{HH}$ = 8.2, 6.0 Hz, 1H, CH_{PYA}), 7.65 (ddd, $^3J_{HH}$ = 7.5, 5.2, $^4J_{HH}$ = 1.5 Hz, 1H, CH_{pyr}), 4.35 (s, 3H, NCH_3), 2.27 (s, 3H, Pd−$NCCH_3$), 0.89 (s, 3H, Pd−CH_3). $^{13}C\{^1H\}$ NMR (100 MHz, CD_2Cl_2): δ 156.9 (CH_{pyr}), 143.9 (CH_{PYA}), 137.9 (CH_{PYA}), 128.1 (CH_{pyr}), 127.3 (CH_{PYA}), 126.6 (CH_{pyr}), 126.0 (CH_{PYA}), 125.6 (CH_{pyr}), 49.3 (NCH_3), 3.7 (Pd−$NCCH_3$), 1.2 (Pd−CH_3). Spectroscopic data for the cis isomer are as follows. ^{1}H NMR (300 MHz, CD_2Cl_2): δ 9.06 (s, 1H, CH_{PYA}), 8.42−8.39 (m, 1H, CH_{pyr}), 8.17−8.12 (m, 2H, CH_{PYA} + CH_{pyr}), 8.09 (d,$^3J_{HH}$ = 6.1 Hz, 1H, CH_{PYA}), 8.06 (t, $^3J_{HH}$ = 7.7, Hz, 1H, CH_{pyr}), 7.85 (dd, $^3J_{HH}$ = 7.7, 5.2 Hz, 1H, CH_{PYA}), 7.55 (ddd, $^3J_{HH}$ = 7.5, 5.7, $^4J_{HH}$ = 1.7 Hz, 1H, CH_{pyr}), 4.33 (s, 3H, NCH_3), 2.44 (s, 3H, Pd−$NCCH_3$), 0.32 (s, 3H, Pd−CH_3). $^{13}C\{^1H\}$ NMR (100 MHz, CD_2Cl_2): δ 150.8 (CH_{pyr}), 144.7 (CH_{PYA}), 141.4 (CH_{PYA}), 140.4 (CH_{pyr}), 130.9 (CH_{pyr}), 136.9 (CH_{PYA}), 125.5 (CH_{PYA}), 127.2 (CH_{pyr}), 49.0 (NCH_3), 4.2 (Pd−$NCCH_3$), −0.5 (Pd−CH_3).

Compound ***9***. Compound **9** was prepared according to the general procedure from **6**. Yield: 85 mg, 65%. HR-MS: m/z calculated for $C_{15}H_{17}N_4OPd$ $[M - PF_6]^+$, 375.0437; found, 375.0418. Spectroscopic data for the trans isomer are as follows. ^{1}H NMR (300 MHz, CD_2Cl_2): δ 8.45−8.40 (m, 2H, CH_{pyr} + CH_{PYA}), 8.23 (dd, $^3J_{HH}$ = 8.0, $^4J_{HH}$ = 1.6 Hz, 1H, CH_{PYA}), 8.19 (td, $^3J_{HH}$ = 8.4, $^4J_{HH}$ = 1.4 Hz, 1H, CH_{pyr}), 8.15−8.12 (m, 1H, CH_{PYA}), 7.78 (dd, $^3J_{HH}$ = 8.4, $^4J_{HH}$ = 1.7 Hz, 1H, CH_{pyr}), 7.66 (dd, $^3J_{HH}$ = 8.0, $^4J_{HH}$ = 1.6 Hz, 1H, CH_{PYA}), 7.44 (td, $^3J_{HH}$ = 8.4, $^4J_{HH}$ = 1.4 Hz, 1H, CH_{pyr}), 4.24 (s, 3H, NCH_3), 2.16 (s, 3H, Pd−$NCCH_3$), 1.01 (s, 3H, Pd−CH_3). $^{13}C\{^1H\}$ NMR (100 MHz, CD_2Cl_2): δ 167.5 (CO), 160.0 (C_{pyr}), 155.6 (C_{PYA}), 147.6 (CH_{pyr}), 144.5 (CH_{pyr}), 143.9 (CH_{PYA}), 140.6 (CH_{PYA}), 128.3 (CH_{PYA}), 127.3 (CH_{PYA}), 126.3 (CH_{pyr}), 121.0 (CH_{pyr}), 44.4 (NCH_3), 3.2 (Pd−$NCCH_3$), 2.6 (Pd−CH_3). Spectroscopic data for the cis isomer are as follows. ^{1}H NMR (300 MHz, CD_2Cl_2): δ 8.47 (dt, $^3J_{HH}$ = 5.0, $^4J_{HH}$ = 1.6 Hz, 1H, CH_{pyr}), 8.45−8.40 (m, 1H, CH_{PYA}), 8.33 (td, $^3J_{HH}$ = 7.3, $^4J_{HH}$ = 1.6 Hz, 1H, CH_{pyr}), 8.12−8.07 (m, 2H, CH_{pyr} + CH_{PYA}), 7.72 (ddd, $^3J_{HH}$ = 7.3, 5.0, $^4J_{HH}$ = 1.6 Hz, 1H, CH_{pyr}), 7.66 (dd, $^3J_{HH}$ = 8.4, $^4J_{HH}$ = 1.4 Hz, 1H, CH_{pyr}), 7.64−7.60 (m, 1H, CH_{PYA}), 4.19 (s, 3H, NCH_3), 2.45 (s, 3H, Pd−$NCCH_3$), 0.10 (s, 3H, Pd−CH_3). $^{13}C\{^1H\}$ NMR (100 MHz, CD_2Cl_2): δ 171.5 (CO), 160.2 (C_{pyr}), 150.5 (C_{PYA}), 148.3 (CH_{pyr}), 145.9 (CH_{pyr}), 144.1 (CH_{PYA}), 140.2 (CH_{pyr}), 129.1 (CH_{PYA}), 129.1 (CH_{pyr}), 125.9 (CH_{PYA}), 123.2 (CH_{PYA}), 121.9 (C_{CH3CN}), 44.4 (NCH_3), 3.9 (Pd−$NCCH_3$), −5.0 (Pd−CH_3).

General Procedure for the Formation of Palladium Complexes 10−12. Compounds **7−9** were dissolved in deuterated DMSO to afford **10−12** with the presence of only the cis isomer. The complexes were only characterized spectroscopically.

Compound ***10***. ^{1}H NMR (300 MHz, d_6-DMSO): δ 9.25 (d, $^3J_{HH}$ = 5.2 Hz, 1H, CH_{pyr}), 8.71 (d, $^3J_{HH}$ = 6.5 Hz, 2H, CH_{PYA}), 8.25 (td, $^3J_{HH}$ = 7.7, $^4J_{HH}$ = 1.6 Hz, 1H, CH_{pyr}), 8.16 (dt, $^3J_{HH}$ = 7.7, $^4J_{HH}$ = 1.6 Hz, 1H, CH_{pyr}), 7.85 (ddd, $^3J_{HH}$ = 7.7, 5.2, $^4J_{HH}$ = 1.6 Hz, 1H, CH_{pyr}), 7.75 (d, $^3J_{HH}$ = 6.5, 2H, CH_{PYA}), 4.21 (s, 3H, NCH_3), 0.17 (s, 3H, Pd−CH_3). $^{13}C\{^1H\}$ NMR (100 MHz, d_6-DMSO): δ 169.6 (CO), 162.8 (C_{PYA}), 151.9 (C_{pyr}), 148.9 (CH_{pyr}), 144.6 (CH_{PYA}), 140.4 (CH_{pyr}), 128.0 (CH_{pyr}), 125.5 (CH_{PYA}), 125.3 (CH_{pyr}), 46.4 (NCH_3), 1.1 (Pd−CH_3).

Compound ***11***. ^{1}H NMR (300 MHz, d_6-DMSO): δ 9.24 (d, $^3J_{HH}$ = 5.2 Hz, 1H, CH_{pyr}), 8.85 (s, 1H, CH_{PYA}) 8.69 (d, $^3J_{HH}$ = 6.0 Hz, 1H, CH_{PYA}), 8.24 (td, $^3J_{HH}$ = 7.7, $^4J_{HH}$ = 1.6 Hz, 1H, CH_{pyr}), 8.19 (d, $^3J_{HH}$ = 8.4 Hz, 1H, CH_{PYA}), 8.12 (d, $^3J_{HH}$ = 7.7 Hz, 1H, CH_{pyr}), 8.06 (dt, $^3J_{HH}$ = 8.4, 6.0 Hz, 1H, CH_{PYA}), 7.85 (ddd, $^3J_{HH}$ = 7.7, 5.2, $^4J_{HH}$ = 1.6 Hz, 1H, CH_{pyr}), 4.35 (s, 3H, NCH_3), 0.05 (s, 3H, Pd−CH_3). $^{13}C\{^1H\}$ NMR (100 MHz, d_6-DMSO): δ 170.3 (CO), 151.8 (C_{PYA}), 149.0 (CH_{pyr}), 147.4 (C_{pyr}), 144.2 (CH_{PYA}), 143.7 (CH_{PYA}), 140.4 (CH_{pyr}), 140.4 (CH_{PYA}), 127.9 (CH_{pyr}), 126.8 (CH_{PYA}), 124.9 (CH_{pyr}), 44.7 (NCH_3), 1.1 (Pd−CH_3).

Compound ***12***. ^{1}H NMR (300 MHz, d_6-DMSO): δ 9.22 (bs, 1H, CH_{pyr}), 8.93 (bs, 1H, CH_{PYA}) 8.51 (bs, 1H, CH_{PYA}), 8.29 (t, $^3J_{HH}$ = 7.8 Hz, 1H, CH_{pyr}), 8.15 (d, $^3J_{HH}$ = 7.8 Hz, 1H, CH_{pyr}), 7.91 (t, $^3J_{HH}$ = 7.8 Hz, 1H, CH_{pyr}), 7.83 (bs, 1H, CH_{PYA}), 7.88 (d, $^3J_{HH}$ = 8.3 Hz, 1H, CH_{PYA}), 4.17 (s, 3H, NCH_3), − 0.12 (s, 3H, Pd−CH_3). $^{13}C\{^1H\}$ NMR (100 MHz, d_6-DMSO): δ 158.6 (C_{PYA}), 150.4 (C_{pyr}), 149.8 (CH_{pyr}), 146.1 (CH_{PYA}), 144.7 (CH_{PYA}), 141.0 (CH_{pyr}), 128.2 (CH_{pyr}), 127.9 (CH_{PYA}), 125.6 (CH_{PYA}), 123.1 (CH_{PYA}), 43.1 (NCH_3), 1.1 (Pd−CH_3).

Ethylene/Methyl Acrylate (MA) Copolymerization Reactions. All catalytic experiments were performed using a Büchi "tinyclave" reactor equipped with an interchangeable 50 mL glass vessel. The vessel was loaded with the desired complex (21 μmol), TFE (21 mL) or distilled CH_2Cl_2 (22 mL), and MA (1.13 mL). The reactor was then placed in a preheated oil bath and connected to the ethylene tank. Ethylene was bubbled for 10 min, and the reactor was pressurized. The reaction mixture was stirred at constant temperature. After the appropriate time, the reactor was cooled to room temperature and vented. An aliquot (200 μL) of the reaction mixture was withdrawn and diluted in MeOH (1 mL) for GC-MS analysis. The reaction mixture was poured into a 50 mL round-bottomed flask with the CH_2Cl_2 (3 × 1 mL) used to wash the glass vessel. Volatiles were removed under reduced pressure, and the residue was dried to constant weight and analyzed by using NMR spectroscopy.

Quantification of the low-molecular-weight products from coplymerization reactions was performed by GC-MS using an Agilent GC 7890 instrument equipped with a DB-225 ms column (J&W, 60 m, 0.25 mm i.d., 0.25 mm film) and He as carrier coupled with a 5975 MSD. Before analysis, samples were diluted with methanol, and nonane was added as an internal standard. Quantification of the products (butenes, hexenes, octenes, and methyl pentenoates) was done using adequate standard solutions prepared in 2,2,2-trifluoroethanol/MA and diluted in methanol containing nonane as internal standard. Calibration curves were obtained using at least five points in the concentration range required for accurate determination of the products, with the regression coefficient $R^2 \geq 0.995$. The analysis of each sample was repeated at least four times.

In Situ Ethylene Dimerization Reactions. Ethylene was bubbled for 5 min into a 10 mM solution of palladium complexes **7−9** in CD_2Cl_2 in an NMR tube. Then, ^{1}H NMR spectra were recorded at 298 K immediately afterward and at selected times. For the low-temperature experiments, the tube was cooled to −50 °C (for **7**) and −30 °C (for **8**), respectively. NOESY experiments were performed using the standard parameters and a mixing time of 500 ms.

1-Hexene Dimerization Catalysis. 1-Hexene (19.2 mol, 1.92 mol or 19.2 mmol) was added to a solution of complex **9** (1 mg, 1.92 mmol) in 1 mL of CH_2Cl_2. The reaction mixture was stirred at 30 °C for 18 h. The crude mixture was analyzed by ^{1}H NMR spectroscopy and GC-MS.

Crystal Structure Determination. Crystal data for *trans*-**7** were collected on a Oxford Diffraction SuperNova area-detector diffractometer using mirror optics monochromated Mo Kα radiation (λ = 0.71073 Å) that was Al filtered.[29] The unit cell constants and an orientation matrix for data collection were obtained from a least-squares refinement of the setting angles of reflections in the range 2.5° < θ < 27.8°. A total of 626 frames were collected using ω scans, with 60 + 60 s exposure time, a rotation angle of 1.0° per frame, and a crystal−detector distance of 65.0 mm, at T = 123(2) K. Data reduction was performed using the CrysAlisPro program.[30] The intensities were corrected for Lorentz and polarization effects, and an absorption correction based on the multiscan method using SCALE3 ABSPACK in CrysAlisPro was applied. The structure was solved by direct methods using SHELXS-97 and refined by full-matrix least-squares fitting on F^2 for all data using SHELXL-97.[31] Hydrogen atoms

were added at calculated positions and refined by using a riding model. Anisotropic thermal displacement parameters were used for all non-hydrogen atoms. The PF_6^- anion is orientationally disordered over two sites. The geometries of the two moieties were restrained to be the same. Further crystallographic details are compiled in Table S1. Crystallographic data for this structure have been deposited with the Cambridge Crystallographic Data Centre (CCDC) as supplementary publication number 1841366.

AUTHOR INFORMATION

Corresponding Authors

*E-mail for B.M.: milaniba@units.it.

*E-mail for M.A.: martin.albrecht@dcb.unibe.ch.

ORCID

Miquel Navarro: 0000-0002-5481-1234

Barbara Milani: 0000-0002-4466-7566

Martin Albrecht: 0000-0001-7403-2329

Notes

The authors declare no competing financial interest.

ACKNOWLEDGMENTS

This paper is dedicated to Ernesto Carmona in honor of his career and with deep appreciation for his pioneering and inspiring work. We thank the Swiss National Science Foundation (200021_162868, R'equip projects 206021_128724 and 206021_170755), the European Research Council (CoG 615653), and the Italian MIUR (PRIN 2015, N° 20154 × 9ATP_005) for financial support, as well as COST CM1205 (CARISMA). We thank the group of Chemical Crystallography of the University of Bern for X-ray analyses.

REFERENCES

(1) (a) Ittel, S. D.; Johnson, L. K.; Brookhart, M. Late-metal catalysts for ethylene homo- and copolymerization. *Chem. Rev.* **2000**, *100*, 1169−1204. (b) Britovsek, G. J. P.; Gibson, V. C.; Wass, D. F. The search for new-generation olefin polymerization catalysts: life beyond metallocenes. *Angew. Chem., Int. Ed.* **1999**, *38*, 428−447.

(2) (a) McKnight, A. L.; Waymoth, R. M. Group 4 ansa-cyclopentadienyl-amido catalysts for olefin polymerization. *Chem. Rev.* **1998**, *98*, 2587−2598. (b) Gibson, V. C.; Spitzmesser, S. K. Advances in non-metallocene olefin polymerization catalysis. *Chem. Rev.* **2003**, *103*, 283−316. (c) Boffa, L. S.; Novak, B. M. Copolymerization of polar monomers with olefins using transition-metal complexes. *Chem. Rev.* **2000**, *100*, 1479−1494. (d) Nakamura, A.; Ito, S.; Nozaki, K. Coordination-insertion copolymerization of fundamental polar monomers. *Chem. Rev.* **2009**, *109*, 5215−5244. (e) Berkefeld, A.; Mecking, S. Coordination copolymerization of polar vinyl monomers H_2C = CHX. *Angew. Chem., Int. Ed.* **2008**, *47*, 2538−2542. (f) Dong, J.-Y.; Hu, Y. Design and synthesis of structurally well-defined functional polyolefins via transition metal-mediated olefin polymerization chemistry. *Coord. Chem. Rev.* **2006**, *250*, 47−65.

(3) Johnson, L. K.; Killian, C. M.; Brookhart, M. New Pd(II)- and Ni(II)-based catalysts for polymerization of ethylene and α-olefins. *J. Am. Chem. Soc.* **1995**, *117*, 6414−6415.

(4) Drent, E.; van Dijk, R.; van Ginkel, R.; van Oort, B.; Pugh, R. I. Palladium catalysed copolymerisation of ethene with alkylacrylates: polar comonomer built into the linear polymer chain. *Chem. Commun.* **2002**, 744−745.

(5) (a) Guironnet, D.; Roesle, P.; Rünzi, T.; Göttker-Schnetmann, I.; Mecking, S. Insertion Polymerization of Acrylate. *J. Am. Chem. Soc.* **2009**, *131*, 422−423. (b) Vela, J.; Lief, G. R.; Shen, Z.; Jordan, R. F. Ethylene Polymerization by Palladium Alkyl Complexes Containing Bis(aryl)phosphino-toluenesulfonate Ligands. *Organometallics* **2007**, *26*, 6624−6635. (c) Luo, S.; Vela, J.; Lief, G. R.; Jordan, R. F. Copolymerization of Ethylene and Alkyl Vinyl Ethers by a (Phosphine-sulfonate)PdMe Catalyst. *J. Am. Chem. Soc.* **2007**, *129*, 8946−8947. (d) Kochi, T.; Noda, S.; Yoshimura, K.; Nozaki, K. Formation of Linear Copolymers of Ethylene and Acrylonitrile Catalyzed by Phosphine Sulfonate Palladium Complexes. *J. Am. Chem. Soc.* **2007**, *129*, 8948−8949. (e) Weng, W.; Shen, Z.; Jordan, R. F. Copolymerization of Ethylene and Vinyl Fluoride by (Phosphine-Sulfonate)Pd(Me)(py) Catalysts. *J. Am. Chem. Soc.* **2007**, *129*, 15450−15451. (f) Ito, S.; Munakata, K.; Nakamura, A.; Nozaki, K. Copolymerization of Vinyl Acetate with Ethylene by Palladium/Alkylphosphine−Sulfonate Catalysts. *J. Am. Chem. Soc.* **2009**, *131*, 14606−14607. (g) Carrow, B. P.; Nozaki, K. Transition-Metal-Catalyzed Functional Polyolefin Synthesis: Effecting Control through Chelating Ancillary Ligand Design and Mechanistic Insights. *Macromolecules* **2014**, *47*, 2541−2555. (h) Chen, Y.; Wang, L.; Yu, H.; Zhao, Y.; Sun, R.; Jing, G.; Huang, J.; Khalid, H.; Abbasi, N. M.; Akram, M. Synthesis and application of polyethylene-based functionalized hyperbranched polymers. *Prog. Polym. Sci.* **2015**, *45*, 23−43. (i) Guo, L.; Dai, S.; Sui, X.; Chen, C. Palladium and Nickel Catalyzed Chain Walking Olefin Polymerization and Copolymerization. *ACS Catal.* **2016**, *6*, 428−441. (j) Sui, X.; Hong, C.; Pang, W.; Chen, C. Unsymmetrical α-diimine palladium catalysts and their properties in olefin (co)polymerization. *Mater. Chem. Front.* **2017**, *1*, 967−972. (k) Guo, L.; Liu, W.; Chen, C. Late transition metal catalyzed α-olefin polymerization and copolymerization with polar monomers. *Mater. Chem. Front.* **2017**, *1*, 2487−2494.

(6) (a) Khlebnikov, V.; Meduri, A.; Mueller-Bunz, H.; Montini, T.; Fornasiero, P.; Zangrando, E.; Milani, B.; Albrecht, M. Palladium Carbene Complexes for Selective Alkene Di- and Oligomerization. *Organometallics* **2012**, *31*, 976−986. (b) Khlebnikov, V.; Meduri, A.; Mueller-Bunz, H.; Milani, B.; Albrecht, M. Synthesis of a sterically modulated pyridine−NHC palladium complex and its reactivity towards ethylene. *New J. Chem.* **2012**, *36*, 1552−1555.

(7) Nakano, R.; Nozaki, K. Copolymerization of Propylene and Polar Monomers Using Pd/IzQO Catalysts. *J. Am. Chem. Soc.* **2015**, *137*, 10934−10937.

(8) Tao, W. J.; Nakano, R.; Ito, S.; Nozaki, K. Copolymerization of Ethylene and Polar Monomers by Using Ni/IzQO Catalysts. *Angew. Chem., Int. Ed.* **2016**, *55*, 2835−2839.

(9) (a) Shi, Q.; Thatcher, R. J.; Slattery, J.; Sauari, P. S.; Whitwood, A. C.; McGowan, P. C.; Douthwaite, R. E. Synthesis, Coordination Chemistry and Bonding of Strong N-Donor Ligands Incorporating the 1H-Pyridin-(2E)-Ylidene (PYE) Motif. *Chem. - Eur. J.* **2009**, *15*, 11346−11360. (b) Slattery, J.; Thatcher, R. J.; Shi, Q.; Douthwaite, R. E. Comparison of donor properties of N-heterocyclic carbenes and N-donors containing the 1H-pyridin-(2E)-ylidene motif. *Pure Appl. Chem.* **2010**, *82*, 1663−1671. (c) Thatcher, R. J.; Johnson, D. G.; Slattery, J. M.; Douthwaite, R. E. Charged Behaviour from Neutral Ligands: Synthesis and Properties of N-Heterocyclic Pseudo-amides. *Chem. - Eur. J.* **2012**, *18*, 4329−4336. (d) Boyd, P. D. W.; Wright, L. J.; Zafar, M. N. Extending the Range of Neutral N-Donor Ligands

Available for Metal Catalysts: N-[1-Alkylpyridin-4(1H)-ylidene]-amides in Palladium-Catalyzed Cross-Coupling Reactions. *Inorg. Chem.* **2011**, *50*, 10522−10524.
(10) (a) Leigh, V.; Carleton, D. J.; Olguin, J.; Mueller-Bunz, H.; Wright, L. J.; Albrecht, M. Solvent-Dependent Switch of Ligand Donor Ability and Catalytic Activity of Ruthenium(II) Complexes Containing Pyridinylidene Amide (PYA) N-Heterocyclic Carbene Hybrid Ligands. *Inorg. Chem.* **2014**, *53*, 8054−8060. (b) Donnelly, K. F.; Segarra, C.; Shao, L.-X.; Suen, R.; Mueller-Bunz, H.; Albrecht, M. Adaptive N-Mesoionic Ligands Anchored to a Triazolylidene for Ruthenium-Mediated (De)Hydrogenation Catalysis. *Organometallics* **2015**, *34*, 4076−4068. (c) Navarro, M.; Li, M.; Mueller-Bunz, H.; Bernhard, S.; Albrecht, M. Donor-Flexible Nitrogen Ligands for Efficient Iridium-Catalyzed Water Oxidation Catalysis. *Chem. - Eur. J.* **2016**, *22*, 6740−6745. (d) Navarro, M.; Smith, C. A.; Albrecht, M. Enhanced Catalytic Activity of Iridium(III) Complexes by Facile Modification of C,N-Bidentate Chelating Pyridylideneamide Ligands. *Inorg. Chem.* **2017**, *56*, 11688−11701. (e) Navarro, M.; Li, M.; Bernhard, S.; Albrecht, M. A mesoionic nitrogen-donor ligand: structure, iridium coordination, and catalytic effects. *Dalton Trans* **2018**, *47*, 659−662.
(11) Mesoionic compounds are defined by IUPAC as "dipolar five-(possibly six-) membered heterocyclic compounds in which both the negative and the positive charge are delocalized, for which a totally covalent structure cannot be written, and which cannot be represented satisfactorily by any one polar structure. The formal positive charge is associated with the ring atoms, and the formal negative charge is associated with ring atoms or an exocyclic nitrogen or chalcogen atom". *IUPAC Compendium of Chemical Terminology(-Gold Book)*, 2nd ed.; McNaught, A. D.; Wilkinson, A.; Blackwell Scientific Publications: Oxford, U.K., 1997. XML on-line corrected version: http://goldbook.iupac.org (2006-) created by M. Nic, J. Jirat, B. Kosata; updates compiled by A. Jenkins (ISBN 0-9678550-9-8).
(12) DFT (B3LYP/LANL2DZ) calculations and X-ray diffraction analysis for related iridium complexes having *ortho*-PYA ligands corroborated the twisted arrangement of the PYA ligand proving the minimal contribution of the neutral imine resonance form *vs* the zwitterionic amide form, see: Navarro, M.; Smith, C. A.; Li, M.; Bernhard, S.; Albrecht, M. Optimization of Synthetically Versatile Pyridylidene Amide Ligands for Efficient Iridium-Catalyzed Water Oxidation. *Chem. - Eur. J.* **2018**, *24*, 6386−6398.
(13) Meduri, A.; Montini, T.; Ragaini, F.; Fornasiero, P.; Zangrando, E.; Milani, B. Palladium-Catalyzed Ethylene/Methyl Acrylate Cooligomerization: Effect of a New Nonsymmetric α-Diimine. *ChemCatChem* **2013**, *5*, 1170−1183.
(14) Rosar, V.; Montini, T.; Balducci, G.; Zangrando, E.; Fornasiero, P.; Milani, B. Palladium-Catalyzed Ethylene/Methyl Acrylate Co-Oligomerization: The Effect of a New Nonsymmetrical α-Diimine with the 1,4-Diazabutadiene Skeleton. *ChemCatChem* **2017**, *9*, 3402−3411.
(15) (a) Rosar, V.; Dedeic, D.; Nobile, T.; Fini, F.; Balducci, G.; Alessio, E.; Carfagna, C.; Milani, B. Palladium complexes with simple iminopyridines as catalysts for polyketone synthesis. *Dalton Trans* **2016**, *45*, 14609−14619. (b) Canil, G.; Rosar, V.; Dalla Marta, S.; Bronco, S.; Fini, F.; Carfagna, C.; Durand, J.; Milani, B. Unprecedented Comonomer Dependence of the Stereochemistry Control in Pd-Catalyzed CO/Vinyl Arene Polyketone Synthesis. *ChemCatChem* **2015**, *7*, 2255−2264.
(16) Analogous NMR spectroscopy analysis for complexes **11** and **12** also revealed the presence of only the cis isomer; see Figures S11−S16.
(17) Griffiths, T. R.; Pugh, D. C. Correlations among solvent polarity scales, dielectric constant and dipole moment, and a means to reliable predictions of polarity scale values from current data. *Coord. Chem. Rev.* **1979**, *29*, 129−211.
(18) (a) Rosar, V.; Meduri, A.; Montini, T.; Fini, F.; Carfagna, C.; Fornasiero, P.; Balducci, G.; Zangrando, E.; Milani, B. Analogies and Differences in Palladium-Catalyzed CO/Styrene and Ethylene/Methyl Acrylate Copolymerization Reactions. *ChemCatChem* **2014**, *6*, 2403−2418. (b) Rosar, V.; Meduri, A.; Montini, T.; Fornasiero, P.; Zangrando, E.; Milani, B. The contradictory effect of the methoxy-substituent in palladium-catalyzed ethylene/methyl acrylate copolymerization. *Dalton Trans* **2018**, *47*, 2778−2790.
(19) Guironnet, D.; Roesle, P.; Rünzi, T.; Göttker-Schnetmann, I.; Mecking, S. Insertion Polymerization of Acrylate. *J. Am. Chem. Soc.* **2009**, *131*, 422−423.
(20) Milani, B.; Marson, A.; Scarel, A.; Mestroni, G. Facile Synthesis of New, Stable, Palladium-Ethyl Derivatives Containing Nitrogen-Donor Ligands. *Organometallics* **2004**, *23*, 1974−1977.
(21) Rix, F. C.; Brookhart, M. Energetics of Migratory Insertion Reactions in Pd(II) Acyl Ethylene, Alkyl Ethylene, and Alkyl Carbonyl Complexes. *J. Am. Chem. Soc.* **1995**, *117*, 1137−1138.
(22) (a) Noda, S.; Nakamura, A.; Kochi, T.; Chung, L. W.; Morokuma, K.; Nozaki, K. Mechanistic Studies on the Formation of Linear Polyethylene Chain Catalyzed by Palladium Phosphine−Sulfonate Complexes: Experiment and Theoretical Studies. *J. Am. Chem. Soc.* **2009**, *131*, 14088−14100. (b) Nakano, N.; Chung, L. W.; Watanabe, Y.; Okuno, Y.; Okumura, Y.; Ito, S.; Morokuma, K.; Nozaki, K. Elucidating the Key Role of Phosphine−Sulfonate Ligands in Palladium-Catalyzed Ethylene Polymerization: Effect of Ligand Structure on the Molecular Weight and Linearity of Polyethylene. *ACS Catal.* **2016**, *6*, 6101−6113. (c) Friedberger, T.; Wucher, P.; Mecking, S. Mechanistic Insights into Polar Monomer Insertion Polymerization from Acrylamides. *J. Am. Chem. Soc.* **2012**, *134*, 1010−1018. (d) Neuwald, B.; Ölscher, F.; Göttker-Schnetmann, I.; Mecking, S. Limits of Activity: Weakly Coordinating Ligands in Arylphosphinesulfonato Palladium(II) Polymerization Catalysts. *Organometallics* **2012**, *31*, 3128−3137. (e) Neuwald, B.; Falivene, L.; Caporaso, L.; Cavallo, L.; Mecking, S. Exploring Electronic and Steric Effects on the Insertion and Polymerization Reactivity of Phosphinesulfonato Pd^{II} Catalysts. *Chem. - Eur. J.* **2013**, *19*, 17773−17788. (f) Conley, M. P.; Jordan, R. F. Cis/trans Isomerization of Phosphinesulfonate Palladium(II) Complexes. *Angew. Chem., Int. Ed.* **2011**, *50*, 3744−3746. (g) Zhou, X.; Jordan, R. F. Synthesis, cis/trans Isomerization, and Reactivity of Palladium Alkyl Complexes That Contain a Chelating N-Heterocyclic-Carbene Sulfonate Ligand. *Organometallics* **2011**, *30*, 4632−4642. (h) Zhou, X.; Lau, K.-C.; Petro, B. J.; Jordan, R. F. Cis/trans Isomerization of o-Phosphino-Arenesulfonate Palladium Methyl Complexes. *Organometallics* **2014**, *33*, 7209−7214. (i) Jian, Z.; Falivene, L.; Wucher, P.; Roesle, P.; Caporaso, L.; Cavallo, L.; Göttker-Schnetmann, I.; Mecking, S. Insights into Functional-Group-Tolerant Polymerization Catalysis with Phosphine-Sulfonamide Palladium(II) Complexes. *Chem. - Eur. J.* **2015**, *21*, 2062−2075.
(23) Tognon, A.; Rosar, V.; Demitri, N.; Montini, T.; Felluga, F.; Milani, B. Coordination chemistry to palladium(II) of pyridylbenzamidine ligands and the related reactivity with ethylene. *Inorg. Chim. Acta* **2015**, *431*, 206−218.
(24) Eckstrom, H. C.; Berger, J. E.; Dawson, L. R. Intermolecular effects in solutions of methyl isobutyl ketone in alcohols and fluoroalcohols. *J. Phys. Chem.* **1960**, *64*, 1458−1461.
(25) Scarel, A.; Durand, J.; Franchi, D.; Zangrando, E.; Mestroni, G.; Milani, B.; Gladiali, S.; Carfagna, C.; Binotti, B.; Bronco, S.; Gragnoli, T. Trifluoroethanol: key solvent for palladium-catalyzed polymerization reactions. *J. Organomet. Chem.* **2005**, *690*, 2106−2120.
(26) For leading references, see: (a) Donohoe, T. J.; O'Riordan, T. J. C.; Rosa, C. P. Ruthenium-Catalyzed Isomerization of Terminal Olefins: Applications to Synthesis. *Angew. Chem., Int. Ed.* **2009**, *48*, 1014−1017. (b) Lim, H. J.; Smith, C. R.; RajanBabu, T. V. Facile Pd(II)- and Ni(II)-Catalyzed Isomerization of Terminal Alkenes into 2-Alkenes. *J. Org. Chem.* **2009**, *74*, 4565−4572. (c) Gauthier, D.; Lindhardt, A. T.; Olsen, E. P. K.; Overgaard, J.; Skrydstrup, T. In Situ Generated Bulky Palladium Hydride Complexes as Catalysts for the Efficient Isomerization of Olefins. Selective Transformation of Terminal Alkenes to 2-Alkenes. *J. Am. Chem. Soc.* **2010**, *132*, 7998−8009. (d) Larsen, C. R.; Grotjahn, D. B. Stereoselective Alkene Isomerization over One Position. *J. Am. Chem. Soc.* **2012**, *134*, 10357−10360. (e) Chen, C.; Dugan, T. R.; Brennessel, W. W.; Weix,

D. J.; Holland, P. L. Z-Selective Alkene Isomerization by High-Spin Cobalt(II) Complexes. *J. Am. Chem. Soc.* **2014**, *136*, 945−955. (f) Larionov, E.; Li, H.; Mazet, C. Well-defined transition metal hydrides in catalytic isomerizations. *Chem. Commun.* **2014**, *50*, 9816−9826.

(27) Rülke, R. E.; Ernsing, J. M.; Spek, A. L.; Elsevier, C. J.; van Leeuwen, P. W. N. M.; Vrieze, K. NMR study on the coordination behavior of dissymmetric terdentate trinitrogen ligands on methylpalladium(II) compounds. *Inorg. Chem.* **1993**, *32*, 5769−5778.

(28) (a) Li, Q.; Zhang, S.-Y.; He, G.; Ai, Z.; Nack, W. A.; Chen, G. Copper-Catalyzed Carboxamide-Directed Ortho Amination of Anilines with Alkylamines at Room Temperature. *Org. Lett.* **2014**, *16*, 1764−1767. (b) Subramanian, P.; Indu, S.; Kaliappan, K. P. A One-Pot Copper Catalyzed Biomimetic Route to N-Heterocyclic Amides from Methyl Ketones via Oxidative C−C Bond Cleavage. *Org. Lett.* **2014**, *16*, 6212−6215.

(29) Macchi, P.; Bürgi, H. B.; Chimpri, A. S.; Hauser, J.; Gal, Z. Low-energy contamination of Mo microsource X-ray radiation: analysis and solution of the problem. *J. Appl. Crystallogr.* **2011**, *44*, 763−771.

(30) *CrysAlisPro (Version 1.171.34.44)*; Oxford Diffraction Ltd., Yarnton, Oxfordshire, U.K., 2010.

(31) Sheldrick, G. M. Crystal structure refinement with SHELXL. *Acta Crystallogr., Sect. C: Struct. Chem.* **2015**, *71*, 3−8.